Geobiology

Geobiology (2012), **10**, 496–505 DOI: 10.1111/j.1472-4669.2012.00340.x

Mobile hydrocarbon microspheres from >2-billion-year-old carbon-bearing seams in the South African deep subsurface

G. WANGER,[1] D. MOSER,[2] M. HAY,[3] S. MYNENI,[4] T. C. ONSTOTT[4] AND G. SOUTHAM[5]

[1]*Department of Microbial & Environmental Genomics, J. Craig Venter Institute, La Jolla, CA, USA*
[2]*Division of Earth and Ecosystem Sciences, Desert Research Institute, Las Vegas, NV, USA*
[3]*ARCADIS U.S., Inc., Highlands Ranch, CO, USA*
[4]*Department of Geosciences, Princeton University, Princeton, NJ, USA*
[5]*Department of Earth Sciences, University of Western Ontario, London, ON, Canada*

ABSTRACT

By ~2.9 Ga, the time of the deposition of the Witwatersrand Supergroup, life is believed to have been well established on Earth. Carbon remnants of the microbial biosphere from this time period are evident in sediments from around the world. In the Witwatersrand Supergroup, the carbonaceous material is often concentrated in seams, closely associated with the gold deposits and may have been a mobile phase 2 billion years ago. Whereas today the carbon in the Witwatersrand Supergroup is presumed to be immobile, hollow hydrocarbon spheres ranging in size from <1 μm to >50 μm were discovered emanating from a borehole drilled through the carbon-bearing seams suggesting that a portion of the carbon may still be mobile in the deep subsurface. ToF-SIMS and STXM analyses revealed that these spheres contain a suite of alkane, alkenes, and aromatic compounds consistent with the described organic-rich carbon seams within the Witwatersrand Supergroup's auriferous reef horizons. Analysis by electron microscopy and ToF-SIMS, however, revealed that these spheres, although most likely composed of biogenic carbon and resembling biological organisms, do not retain any true structural, that is, fossil, information and were formed by an abiogenic process.

Received 4 February 2012; accepted 2 July 2012

Corresponding author: G. Wanger, Tel.: 858 200 1845; fax: 858 200 1881; e-mail: gwanger@jcvi.org

INTRODUCTION

From 3.0 to 2.7 Ga, the Witwatersrand Basin of central South Africa was a site of deposition for intra-cratonic sedimentary and volcanic units (Fig. 1). The basal fluvial sediments of the Witwatersrand Supergroup host one of the world's largest gold deposits (Frimmel, 2002). The gold is mainly localized in quartz-pebble conglomerates, or reefs, and is often closely associated with organic carbon within the deposit (Minter, 1976). This organic carbon occurs as mm- to cm-thick seams or mm size nodules within the gold-bearing reefs (Hallbauer, 1975; De Wit *et al.*, 1992; Robb & Meyer, 1995; Gray *et al.*, 1998; Mossman, 1999; Parnell, 1999; Spangenberg & Frimmel, 2001). Although the accumulation of the organic carbon is not of direct economic value, the concentration of gold within the reefs is proportional to the amount of organic carbon therein: approximately 40% of the gold mined in the Witwatersrand Basin is associated with this carbon (Frimmel, 2002). For this reason, the relationship between Witwatersrand Supergroup organic carbon and gold is one of economic significance (Minter, 1976) and has thus been studied extensively (Gray *et al.*, 1998; England *et al.*, 2001, 2002; Spangenberg & Frimmel, 2001; Kremenetsky & Maksimyuk, 2006).

The origin of these carbon seams is also significant to biogeosciences. Much work has been carried out on the organic components within other Archean metasediments, including a series of studies looking at putative organic microfossils and molecular biomarkers (Brocks *et al.*, 1999; Brasier *et al.*, 2002; Tice & Lowe, 2004; Noffke *et al.*, 2006; Schopf, 2006; Ventura *et al.*, 2007; Rasmussen *et al.*, 2008; Pinti *et al.*, 2009; Javaux *et al.*, 2010; Waldbauer *et al.*, 2010). These hydrocarbons are considered remnants of Earth's early, predominantly prokaryotic biosphere (however, see Brocks *et al.*, 1999; Javaux *et al.*, 2010 for evidence of Archean eukaryotes). In the Witwatersrand Basin, the currently accepted model posits that

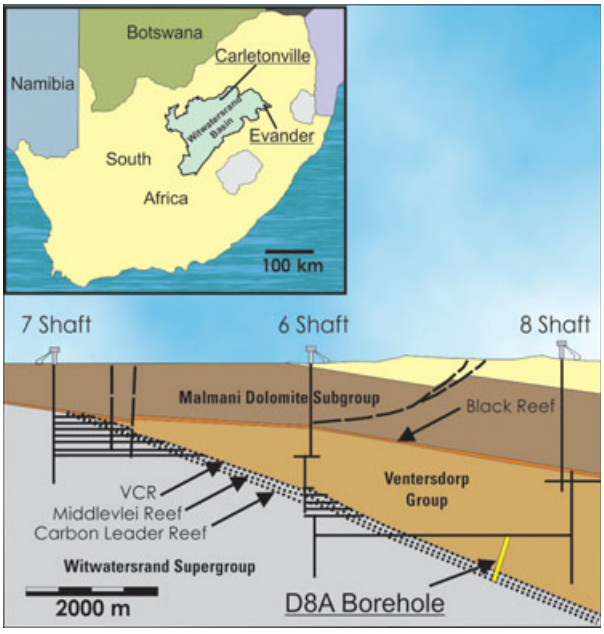

Fig. 1 The Gold Fields Ltd. Driefontein mines are located along the northern margin of the Witwatersrand Basin near the South African town of Carletonville (inset). The 750-m-long borehole D8A emanates from a tunnel floor ~2.7 kmbls intersecting three auriferous reef horizons: the VCR, Middlevlei, and Carbon Leader.

the hydrocarbons are derived from buried kerogens that migrated to their current locations within the reef horizons through porous conduits (Spangenberg & Frimmel, 2001). Although the exact source rock has not been identified, the primary candidate is considered to be within the basin from rock units such as the organic carbon-rich Booysens Shale, which are proximal to commercial reef deposits. According to England *et al.* (2001), the bitumen nodules commonly associated with the reefs formed from the migration of these hydrocarbons through primary zones of porosity (i.e., quartz-pebble conglomerates) within the host rock. Based on petrographic evidence, Parnell (1999) suggested that the emplacement of this hydrocarbon occurred after the deposition of uraninite but prior to the formation of the gold. Radiolytic polymerization has converted the hydrocarbons into the recalcitrant bitumen nodules (Parnell, 1999; England *et al.*, 2001). Although alteration through burial, metamorphism, thermal maturation, migration, and radiolytic polymerization will have likely erased recognizable biological structures over geologic timescales, chemical biosignatures are still detectable in the Witwatersrand Supergroup.

In this study, we present Time of Flight–Secondary ion mass spectrometry (ToF-SIMS) and scanning electron microscopy (SEM) analyses of bitumen nodules from two Witwatersrand Supergroup reefs. We also present ToF-SIMS, electron microscopic and scanning transmission X-ray microscopic analyses of hydrocarbon microspheres discovered in fracture water emanating from a borehole that intersected carbon seams in the Witwatersrand Supergroup. As it is generally believed that the migration of hydrocarbons in the Witwatersrand Basin last occurred at ~2.0 Ga (England *et al.*, 2002), the presence of these microspheres in fracture water that is a few million years old (Moser *et al.*, 2005) poses new questions about the mobility of hydrocarbons in Archean rock units and raises old questions about the interpretation of spherical organic forms as representing biological remains (Buick, 1990).

MATERIALS AND METHODS

Auriferous reef samples

Polished thin sections were prepared from Kimberly Reef and Ventersdorp Contact Reef (VCR) samples. The VCR sample was collected from the Mponeng gold mine (Anglo Gold Ashanti Ltd., Western Levels, Republic of South Africa) in the Carletonville area ~55 km west-southwest of Johannesburg. The Kimberley Reef sample was collected from the Evander gold mine (Harmony Gold Mining Co. Ltd., Evander, Republic of South Africa) in Evander basin ~100 km east of Johannesburg (Fig. 1). The two reef samples were analyzed because of their stratigraphic positioning relative to the Ventersdorp flood basalts and presumed organic-containing metasedimentary horizons below (e.g., Booysens Shale in the case of the Kimberley Reef and Carbon Leader and Middlevlei Reefs in the case of the VCR).

The hydrocarbon microspheres were present in the water collected on October of 2001 from a flowing exploration borehole denoted D8A (Moser *et al.*, 2005) located in an undeveloped sector of the Driefontein gold mine (Gold Fields Ltd.), which is ~3 km northeast of Mponeng gold mine. This sub-vertical (60° from horizontal) 750-m-long borehole had a diameter of 50 mm, below a 10-m-long outlet casing. The hole was diamond cored in 2000 by mine contractors in a horizontal access tunnel at 2.71 km below land surface (kmbls) and reached a depth of 3.36 kmbls. The outlet was located within the Ventersdorp Supergroup; the VCR was intersected at 3.06 kmbls, the Middlevlei Reef at 3.20 kmbls, and the Carbon Leader Reef at 3.34 kmbls. Faults were recorded in the core at 3.28 and 3.30 kmbls. Flowing water was noted upon the completion of coring, and water and gas production rates of 4.5 and 4.6 L min^{-1}, respectively, were measured on 7 November 2001. A minimum of 3×10^6 L of fracture water, or at least 2400 borehole volumes, had flowed from the borehole prior to sample collection of the hydrocarbon microspheres. Fracture water containing carbon microspheres was obtained from 390-m down hole using a bailer as described in (Moser *et al.*, 2005) and fixed with 2% v/v glutaraldehyde following aseptic transfer to 1.5 mL cryovials onsite. The ambient temperature at that depth was

determined to be 54 °C (Moser *et al.*, 2005). The borehole has since been sealed off with cement to quell the flow of water into the mine.

Scanning electron microscopy and focused ion beam milling

Hundred microlitres aliquots of fixed sample water were diluted in 1 mL of deionized water for dispersal and filtered using 0.45 μm isopore membranes (Millipore). The filters were then processed through an ethanol dehydration series (25%, 50%, 75%, 2 × 100% v/v ethanol; 0.5 h for each treatment). The samples were then critical point dried (Samdri PVT 3B, Tousimis, Rockville, MD, USA), sputter coated with metal (Au, Au:Pt alloy or Pt) to prevent charging, and viewed on either a Hitachi S-4500 Field Emission SEM or a Leo 1540 XB FIB/SEM at 10 keV and 5 keV, respectively. Focused ion beam milling was carried out on a Leo 1540 XB FIB/SEM using a Ga^+ ion beam.

Polished geological thin sections were also imaged and analyzed at 20 keV on a Leo 440 SEM equipped with a Gresham light element detector and a Quartz Xone Energy Dispersive X-ray (EDX) analysis system.

Transmission electron microscopy

Glutaraldehyde-fixed samples for ultra-thin sectioning were embedded in 2% (w/v) noble agar and further fixed in 1% (w/v) osmium tetroxide for 1 h and then placed in 2% uranyl acetate (w/v) for 1 h. The samples were dehydrated with an ethanol dehydration series (25%, 50%, 75%, 2 × 100% (v/v) Ethanol; 0.5 h per treatment), then placed in LR-White medium grade acrylic resin (London Resin Co; Reading, England), and allowed to harden overnight at 60 °C. Samples were ultra-thin sectioned (~70 nm) using a Reichert Ultracut E ultramicrotome, and placed on Formvar 15/95 resin (EM Sciences; Fort Washington, PA, USA)-coated copper grids. The sections were post-stained with 2% (w/v) uranyl acetate and 2% (w/v) lead citrate (10 and 2 min, respectively). Examination of the samples was carried out at 60 keV with a Philips EM420 TEM.

Time of Flight–Secondary ion mass spectrometry

The samples for ToF-SIMS, geological reef samples and hydrocarbon spheres, were prepared as described above. ToF-SIMS analysis was carried out at Surface Science Western (University of Western Ontario, London, Canada) using an Ion-ToF (GMBH) ToF-SIMS IV reflectron type mass spectrometer with a pulsed Bi^+ primary beam. Analyses were carried out in high current bunched mode, which offers higher mass resolution at the expense of spatial resolution. A pulsed electron flood gun was used to minimize any charge build up on the sample. A Cs^+ ion beam was used to ion clean the geological samples, providing a fresh surface for analysis. Data were analyzed using the IonSpec™ and Ion-Image™ software suite (Ion-ToF GMBH, Münster, Germany).

Scanning transmission X-ray microscopy

Scanning transmission X-ray microscopy (STXM) analyses were conducted on Beamline 5.3.2 at the Advanced Light Source, Lawrence Berkeley National Laboratory. Samples were air dried onto copper TEM grids and mounted to aluminum sample holders. STXM analyses were performed at the carbon K-edge under He at one atmosphere. The samples were coarsely mapped at an X-ray energy of 290 eV (just above the carbon K-absorption edge) to locate carbon-containing material. Carbon-edge difference maps of the hydrocarbon spheres were then collected at several different locations on the grid. Carbon maps were created by subtracting X-ray images collected below the

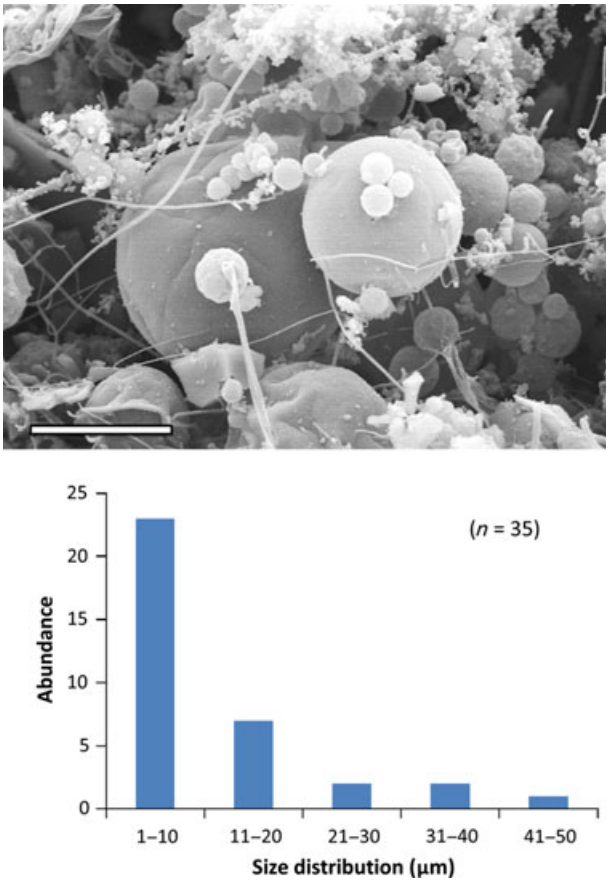

Fig. 2 An SEM micrograph taken of accumulated particulates from a water sample collected from borehole D8A 390 m below the tunnel floor. Spheres of various sizes were observed ranging from <1 μm to >50 μm. The soft material seen surrounding some of the spheres is colloidal silica as determined by EDX. A size distribution of a subset of detected spheres is shown. Bar = 5 μm.

absorption edge at 280 eV from ones collected above the edge at 290 eV. Maps were typically collected with a spatial resolution of 125 nm per pixel and a pixel dwell time of 1.5 ms. Spatially resolved X-ray absorption spectra were collected from the same regions by collecting image 'stacks' as a function of energy, yielding an X-ray absorption spectrum for each pixel within an image. Image stacks were collected between 280 and 320 eV with step sizes of 0.1 eV near the absorption edge (between 283 and 293 eV) and 0.5 eV below and above the edge, a spatial resolution of 60–200 nm per pixel, and a dwell time of 0.5 ms per pixel. X-ray absorption spectra were generated by averaging multiple pixels from within a representative region of the image (e.g., averaging all the pixels within a hydrocarbon sphere) and normalizing with

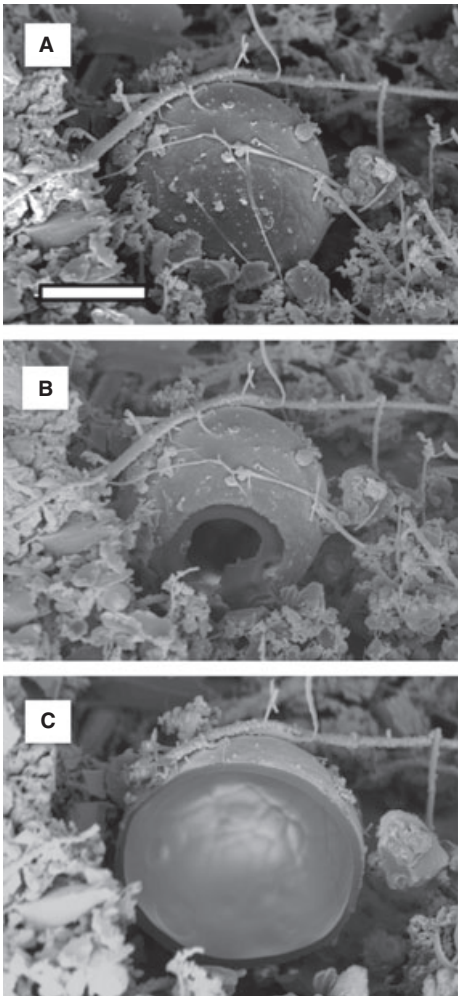

Fig. 3 Several of the spheres appear to be torn (not shown) suggesting they are hollow. Using a focused Ga^+ ion beam, several of the spheres were cut revealing their hollow nature (shown here). The three-image panel (A–C) shows the sphere in the process of being cut open. The low image contrast in the interior of the spheres is most likely due to the lack of the metal coating used to dissipate charge in the electron microscope. Bar = 2 μm.

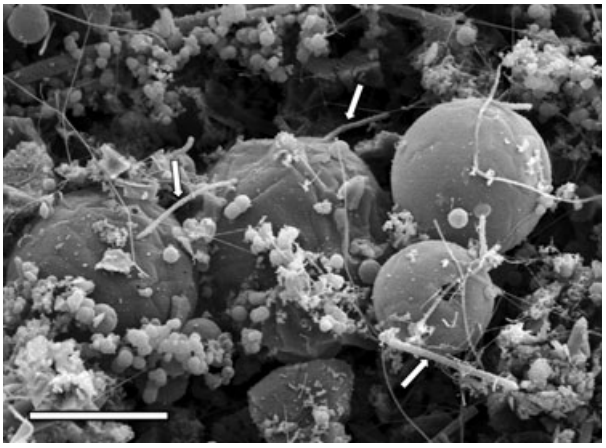

Fig. 4 The micro-organisms observed in the samples (arrows) all possess an elongated rod shape consistent with the inferred morphology of the major microbial form detected in these samples (candidatus *Desulforudis audaxviator* (Moser *et al.*, 2005; Chivian *et al.*, 2008; Supplement). Although in this micrograph the micro-organisms appear to be intimately associated with the spheres, this is likely due to filtering of the samples (Bar = 5 μm).

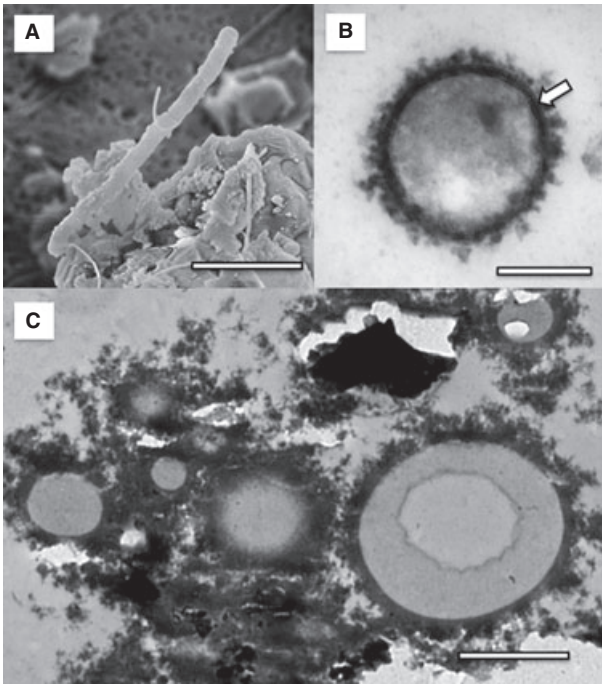

Fig. 5 (A) A scanning electron micrograph showing a micro-organism with the elongated rod morphology typical for this sample (Bar = 1 μm). Using transmission electron microscopy and ultra-thin sectioned samples (B), the micro-organisms show well-defined cell envelopes consistent with a gram-positive wall surrounded by an S-layer (arrow) (Bar = 100 nm), as might be expected for a Firmicute, such as candidatus *Desulforudis audaxviator,* the dominant micro-organism detected in these samples (Moser *et al.*, 2005). Unlike the microbial forms, the spheres do not show any definable ultrastructure (C) (Bar = 10 μm).

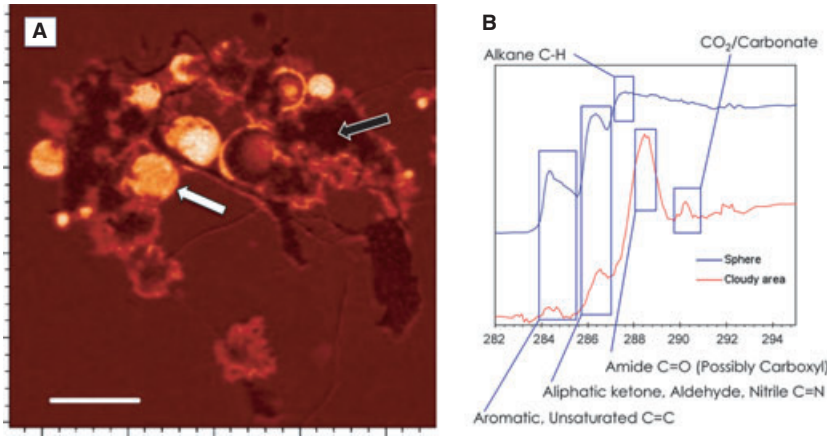

Fig. 6 (A) Carbon K-edge difference map of the hydrocarbon spheres created using STXM (Bar = 5 μm). Lighter areas correspond to higher cross-sectional densities of carbon. (B) X-ray absorption spectra generated from image stacks collected on the same region as in (A). The sphere spectrum represents an average of spectra collected over the entire area of the sphere indicated by the white arrow, while the 'cloudy area' spectrum was generated from multiple spectra collected in the region indicated by the black arrow.

a spectrum generated from a blank, open area within the image. Energy calibration was performed by collecting an absorption spectrum on CO_2 gas introduced into the sample chamber and setting the absorption peak to 290.7 eV.

RESULTS

Scanning electron microscopy micrographs of the water samples collected from borehole D8A show the presence of large numbers of spherical structures (Fig. 2). These spheres vary in size from <1 μm to more than 50 μm and their bulk elemental composition was determined, with SEM-EDX, to be mainly carbon. By its nature, EDX spectra are collected from a 'large' volume of sample owing to the penetration of the electron beam into the sample and therefore these data represent the bulk composition of sample to a depth of ~10 μm. The fine-grained, 10s of nm-scale 'soft' materials seen in the micrograph are silica colloids, which presumably precipitated as a result of the post-sampling temperature drop from 54 °C. Numerous spheres appear torn suggesting that the spheres, at least the larger ones, are hollow. This hypothesis was confirmed by focused ion beam (FIB) milling of several intact spheres, which revealed their hollow nature (Fig. 3). The low image contrast observed in the interior of the spheres is owing to the lack of a metal coating to dissipate the charge of the electron beam.

Forms that appear to be intact micro-organisms were also observed in the samples from the D8A (arrows in Fig. 4). All micro-organisms observed appeared to share the same morphology, an extended rod shape between 3–10 μm in length and 0.3 μm wide (Fig. 4, arrows). Although the micro-organisms and the hydrocarbon spheres in Fig. 4 appear to be closely associated, this was not always the case (data not shown). This observation is supported by the use of TEM, which showed that cells were not directly associated with the spheres (Figs 2–5). TEM ultra-thin sections also indicated that the spheres

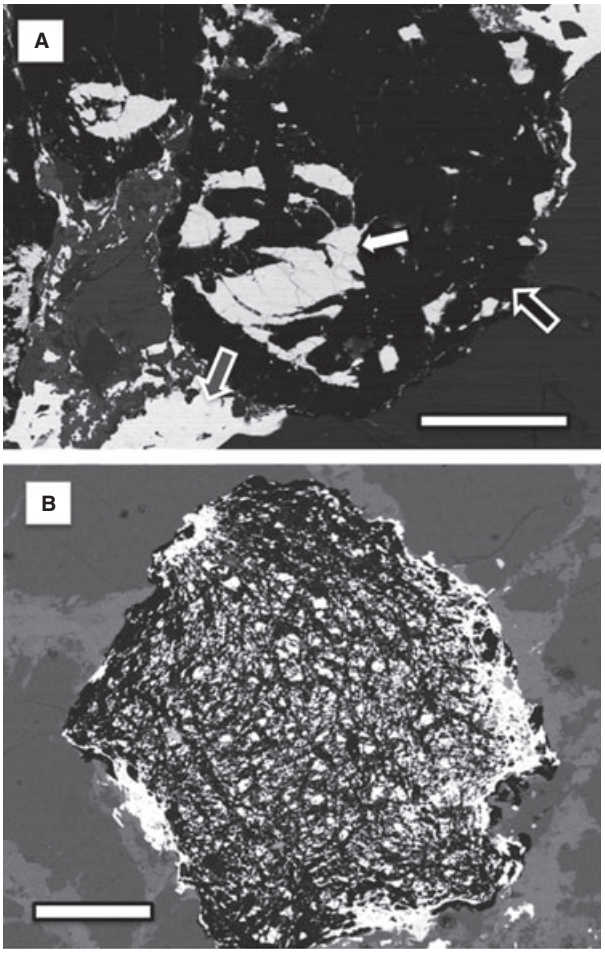

Fig. 7 Backscatter SEM micrographs of polished, geological thin sections of carbon nodules from the Kimberley Reef (A) and VCR (B). The contrast in these images is generated from differences in the average atomic number (i.e., higher atomic mass = lighter shades). The Kimberley Reef sample (A) shows a rounded uraninite grain (white arrow) encased in hydrocarbons (black arrow). The gold in this sample was always observed external to the hydrocarbons (gray arrow) supporting the proposed depositional timeline from oldest to youngest of uraninite, then hydrocarbons, and finally gold. The VCR carbon shows more post-depositional alteration in that the uraninite is highly fragmented.

were not biological. Whereas micro-organisms within the same samples (Fig. 5A) exhibited a clearly defined gram-positive cell envelope with an S-layer when observed by TEM in ultra-thin section (Fig. 5B), the spheres (Fig. 5C) lack any such defined envelope suggesting that they are not cellular in nature. STXM analyses indicated that the spheres were a mixture of hydrocarbon species including alkanes and aromatics (Fig. 6). The XANES spectrum of the spheres (Fig. 6A, white arrow) also show features suggestive of aliphatic ketones, aldehyde, or nitrile groups. The 'soft' mixture of silica colloids, filaments, and cells outside of the hydrocarbon spheres (Fig. 6B, black arrow) yielded a large peak in the XANES spectrum consistent with amides or possibly carboxyl groups and carbonate.

Scanning electron microscopy-EDX analyses of the Kimberley Reef revealed hydrocarbons (black arrow in Fig. 7A) enveloping a rounded uraninite grain (white arrow in Fig. 7A). In this sample, the gold (gray arrow in Fig. 7A) is concentrated on the exterior of the polymerized hydrocarbons. The carbon nodules within the VCR reef sample (Fig. 7B), although similar to the Kimberley Reef nodules, appear as flyspeck nodules and the highly fragmented uraninite suggests a higher degree of post-depositional alteration. Although gold visible to the naked eye was observed in the corresponding hand specimen, this particular thin section does not possess any particles of gold such as those observed in the Kimberley Reef sample.

To compare the compositional structure of the hydrocarbon nodules in the VCR and Kimberley Reef with that of the spheres, ToF-SIMS analyses were performed on all three. ToF-SIMS can map the constituents of a sample but unlike the EDX, the ToF-SIMS allows for the collection of both mono- and poly-atomic ions.

Time of Flight-SIMS ion spectra for the VCR and Kimberly Reef samples revealed many of the same constituents (Fig. 8). Although the D8A borehole did not intersect the Kimberley Reef, samples from it were analyzed because of its stratigraphic proximity to the Booysens Shale, one of the postulated source rocks for the hydrocarbons. Both samples revealed a suite of low molecular weight polyatomic ions ($m/z < 100$ AMU) consistent with short-chain alkanes, alkenes, and arenes (Fig. 8A). At higher atomic masses, similar arrays of peaks consistent with more complex organic molecules can also be resolved including aromatic and polyaromatic compounds such as toluene (m/z 92.06),

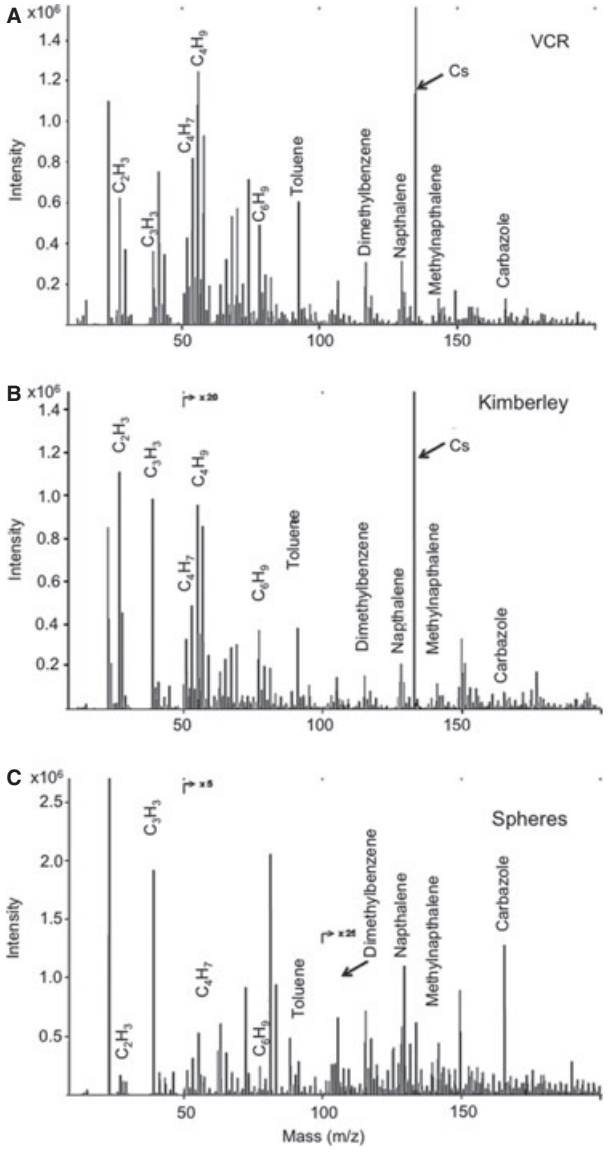

Fig. 8 Time of Flight-SIMS ion spectra from the VCR, Kimberley Reef, and hydrocarbon spheres. These spectra show similarities suggesting that the spheres have their origin in one or multiple organic-rich reef horizons. The spectra show ions consistent with alkanes, alkenes, and arenes. The large Cs peak seen in the geological samples is from sputtering these samples prior to analysis to clean the surface.

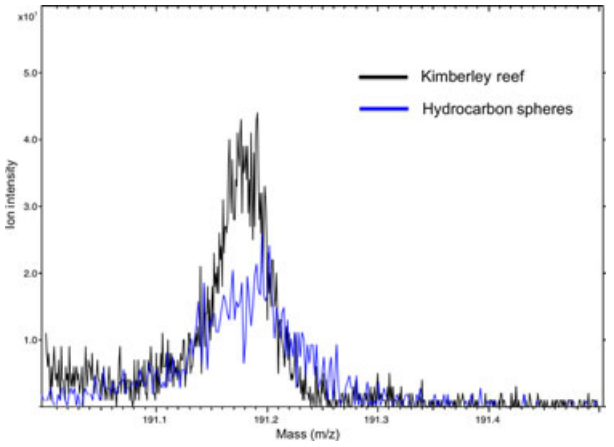

Fig. 9 Detail ToF-SIMS ion spectra from VCR and hydrocarbon spheres. The m/z 191.18 ion is a dominant peak associated with hopane biomarkers. The m/z 191.18 peaks from the VCR and spheres support a biogenic origin for the carbon seams in the Witwatersrand and a similarity between the spheres and the seam hydrocarbons.

dimethylbenzene (m/z 106.08), naphthalene (m/z 128.07), methylnaphthalene (m/z 142.09), and carbazole (m/z 166.05). The large Cs peak in both reef samples is attributed to the sputtering of the geological samples with Cs^+ to clean off surface contaminants prior to analysis.

Although there are some differences in relative abundance, the ion spectrum from the hydrocarbon spheres exhibited low molecular weight alkane, alkene, and aromatic profiles similar to those of the geological samples. The co-appearance of peaks in all three samples consistent with toluene, dimethylbenzene, naphthalene, and carbazole suggests that these spheres may have originated from one or more of the hydrocarbon-bearing reef horizons intersected by the D8A borehole (i.e., VCR, Middlevlei reef, and/or the Carbon Leader Reef). The spectrum derived from the hydrocarbon spheres and the Kimberley Reef revealed a peak at m/z 191.18 (Fig. 9), which is consistent with an ion derived from hopanes, common biomarkers in Phanerozoic geological samples and even found in early Proterozoic oil-bearing fluid inclusions (Dutkiewicz *et al.*, 1998).

DISCUSSION

Many researchers have proposed that the hydrocarbons associated with Witwatersrand Basin ore deposits originated from post-burial heating of organic matter and the subsequent migration of maturing hydrocarbons (Buick *et al.*, 1998; Spangenberg & Frimmel, 2001; England *et al.*, 2002). Although an early report suggested plant origins (Hallbauer, 1975) for the carbon, the ~2.9 Ga. depositional age of the Witwatersrand Supergroup predates the first known plant life (Kenrick & Crane, 1997). Today, a more commonly accepted hypothesis is that the Witwatersrand Supergroup organic carbon is prokaryotic in origin (Gray *et al.*, 1998; England *et al.*, 2001).

Regardless, once buried, biomass would begin to decompose and, with continued burial causing the temperature and pressure of surrounding sediments to increase, would undergo diagenesis. At relatively low temperatures, nucleic acids and proteins decompose, whereas lipids and other structural components of cells remain relatively unchanged. At higher temperatures, the buried organics would enter what is known as the oil window (60–150 °C) (Tissot & Welte, 1984; Hunt, 1996). At these temperatures, buried kerogen (organic matter) would begin to form conventional petroleum and most structural (i.e., fossil) information would be lost. Only molecular fossils and other indirect evidence for a biogenic origin would remain. Above 200 °C, hydrocarbon formation enters a 'destructive' phase where it is cracked to CH_4 and graphite (Tissot & Welte, 1984; Hunt, 1996). The presence of small, 5–10 μm, petroleum-bearing fluid inclusions, and CH_4-N_2-rich gas fluid inclusions 5–30 μm in size in the Witwatersrand Supergroup quartzite confirms that petroleum and methane were migrating through the formations between 2.3 and 2.0 Ga (Dutkiewicz *et al.*, 1998; Drennan *et al.*, 1999). Dutkiewicz *et al.* (1998) speculated that the closed system behavior of the fluid inclusions was responsible for the survival of these petroleum fluids even after they had experienced peak metamorphic temperatures of >300 °C.

In the Witwatersrand Basin, Parnell (1999) used evidence from petrography to suggest an emplacement history for these deposits, which in order from the oldest to the youngest is uraninite, then hydrocarbons, and finally gold. The nodules observed in the VCR and Kimberley Reefs (Fig. 7) support this interpretation. The rounded nature of the uraninite particles within the Kimberley Reef sample (Fig. 7A) is consistent with the hypothesis that the uraninite is of detrital origin and was most likely syndepositional with its hostpebble conglomerate at time when atmospheric pO_2 was low. The fact that the Kimberly Reef gold is largely restricted to the exterior of hydrocarbon nodules further supports the interpretation that the gold was emplaced after hydrocarbon deposition (England *et al.*, 2001). Conversely, the VCR reef (Fig. 7B) diverges from this paradigm in that the uraninite appears as smaller particles within the hydrocarbon matrix and the hydrocarbons appear to have been reworked after the deposition of the gold.

Kremenetsky & Maksimyuk (2006) reported that bitumens from around the Witwatersrand Basin contain a complex suite of hydrocarbons that include alkanes, alkenes, and aromatics such as naphthalene, phenanthrene, and chrysene and that the aromatics made up a significant portion of the hydrocarbons. Specifically in the VCR, aromatic hydrocarbons comprised between 24.2% and 61.2% of the total organic content (Kremenetsky & Maksimyuk, 2006). This is consistent with the proposed intrabasinal derivation of the hydrocarbons put forth by Spangenberg & Frimmel (2001). Our ToF-SIMS analyses of the hydrocarbons in the Kimberley Reef and VCR revealed a similar suite of alkane, alkene, and aromatic compounds, such as naphthalene and other larger polycyclic aromatic compounds. The similarities of the ion spectra (Fig. 8A–C) and the STXM data (Fig. 7) from the hydrocarbon spheres to both the Kimberley Reef and VCR support the hypothesis that the organic matter forming the spheres has experienced the same geological history as the hydrocarbon-rich zones of the Witwatersrand Supergroup sedimentary assemblage. ToF-SIMS spectra from all three sources show similar profiles of low molecular weight compounds and all three samples contain ions consistent with aromatic and polycyclic aromatic hydrocarbons such as benzene, naphthalene, and carbazole (Fig. 8A–C). Likewise, fragments consistent with hopanes (Steele *et al.*, 2001) like the m/z 191.18 hopane marker (Fig. 9) were also observed within both reefs and spheres, suggesting a primary source for the hydrocarbons may be Archean bacterial mats or marine planktonic communities. De Grego-

rio *et al.* (2009), using STXM at the carbon absorption edge, reported a suite of carbonaceous materials (e.g., aromatic hydrocarbons, etc.) in both the 1.9 Ga Gunflint Chert and 3.5 Ga Apex Chert similar to that observed in D8A spheres. They concluded that this ancient carbon was biogenic in origin, but it had been hydrothermally degraded and transported to its current location within the formation (De Gregorio *et al.*, 2009). The spheres observed in the D8A borehole may represent a similar migration of hydrothermally altered carbon.

According to Moser *et al.* (2005), 12 months of continuous flow from borehole D8A had effectively flushed any drilling-associated chemical and microbial contaminants from the borehole by the time our samples were collected. Microbial profiles in subsamples of the same water samples used in this study revealed a very simple community comprised almost entirely of deeply branching (16S *rRNA* and *dsrAB* gene profiling) Firmicutes related to *Desulfotomaculum spp* and some relatively rare archaea related to *Methanobacterium* spp (16S rRNA and *mcrA*) (Moser *et al.*, 2005). This result is strongly consistent with the correspondingly low diversity of apparent microbial morphologies noted in Fig. 4. The Firmicute lineage is now known as candidatus *Desulforudis audaxviator* and has become widely accepted as a bona fide deep subsurface microorganism (Lin *et al.*, 2006; Chivian *et al.*, 2008). When considered in light of the fact that the spheres were not detected in numerous more poorly flushed holes studied during the Witwatersrand research project (data not shown; Onstott *et al.*, 2006; Moser *et al.*, 2003), the microbial dataset is most consistent with a subsurface origin for the spheres, most likely from one or more of the three carbon-rich auriferous reef horizons intersected by the borehole.

Mechanistically, the intersection of carbon-rich reef horizons by borehole D8A and the effect of the large volume of warm (~54 °C) water emanating from fractures cross-cutting the reefs (especially the Middlevlei Reef, Moser *et al.*, 2005) probably caused the liberation of at least a portion of the emplaced hydrocarbons, manifesting as hollow spheres (Figs 2–4) that emanated from the deeper portions of the slowly upwardly flowing borehole water column. SEM micrographs show a large size distribution of the spheres, ranging from sub-micron to larger than 50 μm (Fig. 2 inset). The hollow nature of at least some of the hydrocarbon spheres (Fig. 3) suggests a mechanism involving the exsolution and expansion of gas or, perhaps, lighter hydrocarbons affected by the pressure decrease associated with release from the formation and subsequent movement up the borehole water column. The interface between the VCR and the D8A borehole is approximately 350 m below the mine tunnel, whereas the Carbon Leader Reef intersection lies more than 630 m below the tunnel (see Fig. 1 and Moser *et al.*, 2005). The up-flowing water, and any suspended particles therein, undergo a pressure decrease of approximately 3.5 MPa and 6.3 MPa from the VCR and Carbon Leader, respectively. At a pressure decrease of 6.3 MPa, a volume of gas will expand ~57 times its original volume, assuming ~110 kPa of air pressure at 2.7 kmbls. Any volatile or dissolved gases within the spheres would thus expand resulting in hollow spheres. If this proposed mechanism is correct, then hollow hydrocarbon spheres should be a common occurrence in hydrothermal systems and the potential for trapping these spheres in chert and quartz veins (in this case via silica colloids) would exist. The lesson learnt from the hydrocarbon spheres of the D8A borehole should be that hollow hydrocarbon spheres, even those bearing biomarkers, do not necessarily represent ancient micro-organisms.

The compositional similarity of the hydrocarbon spheres to the reef carbon would support an assertion that they represent remnants of an early biosphere. Further extrapolations based on structural evidence would lead to the false conclusion that they are the preserved remains of ancient 1–50 μm organisms. When considering putative microfossils in geological samples, especially with SEM, extreme caution must be employed because many micron-scale structures from a variety of sources can resemble fossilized micro-organisms (Schopf, 1976; Mckay *et al.*, 1996). The origins of many microfossils, such as those described in the ~3.5 Ga Apex Chert (Schopf & Packer, 1987), have been questioned because plausible, abiotic mechanisms for their formation have been described (Brasier *et al.*, 2002; Pinti *et al.*, 2009; Marshall *et al.*, 2011). One should be especially cautious with spheres of organic carbon as these would tend to form whenever hydrophobic fluids such as hydrocarbons are released in an aqueous phase. These 'oils' would tend to form spheres minimizing surface tension forces. These spheres like other putative microfossils would retain chemical signatures (e.g., biomarkers, isotopic signatures, etc.) of their source material (De Gregorio *et al.*, 2009) but all original structural information would be erased. Hollow carbon spheres, such as those described emanating from the D8A borehole, have even been reported from the Tagish Lake meteorite, which are believed to have formed, in interstellar space, from aqueous alteration of hydrophobic hydrocarbons (Brown *et al.*, 2000; Nakamura *et al.*, 2002; Nakamura-Messenger *et al.*, 2006). TEM, however, can help to show the internal ultrastructure (Southam & Donald, 1999) and when coupled with SEM or other techniques, aid in the identification of true microfossils and microbes such as those seen in this study (Figs 4 and 5).

Although the origin of the carbon comprising the structures under examination in this work appears to be biological, this demonstration of the formation and accumulation of hydrocarbon microspheres in the deep subsur-

face may illuminate processes that would have been important for the organization of early life precursors. The detection of abundant hydrocarbon spheres in hole D8A suggests an ancient mechanism for the formation of liposomes or micelles that if filled with aqueous fluids could become compartments for prebiotic synthesis reactions (Szostak *et al*., 2001). On the prebiotic Earth, it is easy to imagine that above hydrothermal vents and fractures where Fischer–Tropsch synthesis of hydrocarbons was occurring under high pressures, a stream of gas-inflated hydrocarbon vesicles like those described here would rise through a Hadean ocean or crustal aquifer.

The identification of biomarkers within the emplaced hydrocarbons of the Witwatersrand Supergroup auriferous reef horizons is consistent with the theory that their origins lie with the burial of ancient biological material, conversion of that material to petroleum, and finally its migration to the reef horizons. What this study also shows is that while it was commonly believed that the migration of these oils had ceased, a fraction of these hydrocarbons are still mobile, at least under mining-impacted hydrological regimes. One possible explanation for the origin of the mobile hydrocarbons would be by decrepitation of the petroleum-bearing fluid inclusions in the Witwatersrand Supergroup quartzite (Dutkiewicz *et al*., 1998, 2006) and the subsequent migration of this petroleum phase into the fluid-filled fractures. This mechanism is suggested by neon isotope data from the fracture water encountered in the mines of this region, which indicate that it is comprised of noble gases at least 2 billion years old and isotopically identical to that found in fluid inclusions (Lippmann-Pipke *et al*., 2011). Although it remains difficult to establish the exact origins of the hydrocarbon spheres in hole D8A, the coincidence of common markers, such as the suite of arenes (Fig. 8) and the m/z 191.18 hopane marker (Fig. 9), in both the spheres and the reef hydrocarbons suggests that the origins of both are from within the reefs.

CONCLUSIONS

In both this study and that of Moser *et al.* (2005), borehole D8A has proved to be a tremendous window into the terrestrial deep subsurface and perhaps temporally back in time, revealing both aspects of an extant deep microbial ecosystem and organic components that may or may not interact with the modern biosphere. This study also reinforces the need for caution when interpreting the origin of putative microfossils based on morphology. The data presented here show that although the materials making up these structures (i.e., the hydrocarbon spheres) may be of biogenic origin, they do not represent biological entities as we know them. Rather, because they lack the microbial structures that we customarily associate with cellular life (e.g., membranes and cell walls), the real value of these enigmatic forms detected in a little-studied setting may be to reveal abiological aspects of carbon maturation, accumulation, and mobility in the extant deep subsurface and perhaps ancient Earth and beyond.

ACKNOWLEDGMENTS

This work was supported by National Science Foundation LExEn Program grant EAR-9978267 to TC Onstott and in part by an NSERC Discovery grant to G. Southam. We gratefully acknowledge the support of Gold Fields Ltd., Driefontein Consolidated Mine, who granted access to the 9 shaft tunnel and to mine geologist Dawie Nel and mine engineer Ben Kotze. Also, thanks to C. Ralston at Harmony Gold Mining Company Limited for the Kimberley Reef Sample. We also thank the reviewers for their comments and insights.

REFERENCES

Brasier MD, Green OR, Jephcoat AP, Kleppe AK, Kranendonk MJV, Lindsay JF, Steele A, Grassineauk NV (2002) Questioning the evidence for Earth's oldest fossils. *Nature* **416**, 76–81.

Brocks JJ, Logan GA, Buick R, Summons RE (1999) Archean molecular fossils and the early rise of eukaryotes. *Science* **285**, 1033–1036.

Brown PG, Hildebrand AR, Zolensky ME, Grady M, Clayton RN, Mayeda TK, Tagliaferri E, Spalding R, Macrae ND, Hoffman EL, Mittlefehldt DW, Wacker JF, Bird JA, Campbell MD, Carpenter R, Gingerich H, Glatiotis M, Greiner E, Mazur MJ, Mccausland PJ, Plotkin H, Rubak Mazur T (2000) The fall, recovery, orbit, and composition of the Tagish Lake meteorite: a new type of carbonaceous chondrite. *Science* **290**, 320–325.

Buick R (1990) Microfossil recognition in Archean rocks: an appraisal of spheroids and filaments from a 3500 my old chert-barite unit at North Pole, Western Australia. *Palaios* **44**, 1–459.

Buick R, Rasmussen B, Krapez B (1998) Archean oil: evidence for extensive hydrocarbon generation and migration 2.5-3.5 Ga. *AAPG Bulletin-American Association of Petroleum Geologists* **82**, 50–69.

Chivian D, Brodie EL, Alm EJ, Culley DE, Dehal PS, Desantis TZ, Gihring TM, Lapidus A, Lin LH, Lowry SR, Moser DP, Richardson PM, Southam G, Wanger G, Pratt LM, Andersen GL, Hazen TC, Brockman FJ, Arkin AP, Onstott TC (2008) Environmental genomics reveals a single-species ecosystem deep within Earth. *Science* **322**, 275–278.

De Gregorio BT, Sharp TG, Flynn GJ, Wirick S, Hervig RL (2009) Biogenic origin for Earth's oldest putative microfossil. *Geology* **37**, 631–634.

De Wit MJ, Roering C, Hart RJ, Armstrong RA, De Ronde CEJ, Green RWE, Tredoux M, Peberdy E, Hart RA (1992) Formation of an Archaean Continent. *Nature* **357**, 553–562.

Drennan G, Boiron MC, Cathelineau M, Robb L (1999) Characteristics of post-depositional fluids in the Witwatersrand Basin. *Mineralogy and Petrology* **66**, 83–109.

Dutkiewicz A, Rasmussen B, Buick R (1998) Oil preserved in fluid inclusions in Archaean sandstones. *Nature* **395**, 885–888.

Dutkiewicz A, Volk H, George SC, Ridley J, Buick R (2006) Biomarkers from Huronian oil-bearing fluid inclusions: an

uncontaminated record of life before the Great Oxidation Event. *Geology* **34**, 437–440.
England GL, Rasmussen B, Krapez B, Groves DI (2001) The origin of uraninite, bitumen nodules and carbon seams in witwatersrand GOLD-uranium-pyrite ore deposits, based on a Permo-Triassic Analogue. *Economic Geology* **96**, 1907–1920.
England GL, Rasmussen B, Krapez B, Groves DI (2002) Archaean oil migration in the Witwatersrand Basin of South Africa. *Journal of the Geological Society* **159**, 189–201.
Frimmel HE (2002) Genesis of the World's largest gold deposit. *Science* **297**, 1815–1817.
Gray GJ, Lawrence SR, Kenyon K, Cornford C (1998) Nature and origin of 'carbon' in the Archaean Witwatersrand Basin, South Africa. *Journal of the Geological Society* **155**, 39–59.
Hallbauer DK (1975) The Plant Origin of the Witwatersrand "Carbon". *Minerals Science and Engineering* **7**, 111–131.
Hunt JM (1996) *Petroleum Geochemistry and Geology*, WH Freeman, New York, NY.
Javaux EJ, Marshall CP, Bekker A (2010) Organic-walled microfossils in 3.2-billion-year-old shallow-marine siliciclastic deposits. *Nature* **463**, 934–938.
Kenrick P, Crane PR (1997) The origin and early evolution of plants on land. *Nature* **389**, 33.
Kremenetsky AA, Maksimyuk IE (2006) New data on hydrocarbons in auriferous conglomerates of the Witwatersrand ore region, Republic of South Africa. *Lithology and Mineral Resources* **41**, 102–116.
Lin LH, Wang PL, Rumble D, Lippmann-Pipke J, Boice E, Pratt LM, Sherwood Lollar B, Brodie EL, Hazen TC, Andersen GL, Desantis TZ, Moser DP, Kershaw D, Onstott TC (2006) Long-term sustainability of a high-energy, low-diversity crustal biome. *Science* **314**, 479–482.
Lippmann-Pipke J, Sherwood Lollar B, Neidermann S, Stroncik N, Naumann R, Vanheerden E, Onstott TC (2011) Neon identifies two billion year old fluid component in Kaapvaal Craton. *Chemical Geology* **282**, 287–296.
Marshall CP, Emry JR, Marshall AO (2011) Haematite pseudomicrofossils present in the 3.5-billion-year-old Apex Chert. *Nature Geoscience* **4**, 240–243.
Mckay DS, Gibson EK Jr, Thomas-Keprta KL, Vali H, Romanek CS, Clemett SJ, Chillier XDF, Maechling CR, Zare RN (1996) Search for past life on Mars: possible relic biogenic activity in Martian Meteorite ALH84001. *Science* **273**, 924.
Minter WEL (1976) Detrital gold, uranium, and pyrite concentrations related to sedimentology in the Precambrian Vaal Reef placer, Witwatersrand, South Africa. *Economic Geology and the Bulletin of the Society of Economic Geologists* **71**, 157–176.
Moser DP, Onstott TC, Fredrickson JK, Brockman FJ, Balkwill DL, Drake GR, Pfiffner S, White DC, Takai K, Pratt LM, Fong J, Sherwood Lollar B, Slater G, Phelps TJ, Spoelstra N, Deflaun M, Southam G, Welty AT, Baker BJ, Hoek J (2003) Temporal shifts in the Geochemistry and Microbial Community Structure of an Ultradeep Mine Borehole After isolation from Mine Impacts. *Geomicrobiology Journal* **20**, 517–548.
Moser DP, Gihring TM, Brockman FJ, Fredrickson JK, Balkwill DL, Dollhopf ME, Lollar BS, Pratt LM, Boice E, Southam G, Wanger G, Baker BJ, Pfiffner SM, Lin LH, Onstott TC (2005) Desulfotomaculum and Methanobacterium spp. dominate a 4- to 5-kilometer-deep fault. *Applied and Environmental Microbiology* **71**, 8773–8783.
Mossman DJ (1999) Carbonaceous substances in mineral deposits: implications for geochemical exploration. *Journal of Geochemical Exploration* **66**, 241–247.
Nakamura K, Zolensky ME, Tomita S, Nakashima S, Tomeoka K (2002) Hollow organic globules in the Tagish Lake meteorite as possible products of primitive organic reactions. *International Journal of Astrobiology* **1**, 179–189.
Nakamura-Messenger K, Messenger S, Keller LP, Clemett SJ, Zolensky ME (2006) Organic globules in the Tagish Lake meteorite: remnants of the protosolar disk. *Science* **314**, 1439–1442.
Noffke N, Eriksson KA, Hazen RM, Simpson EL (2006) A new window into Early Archean life: Microbial mats in Earth's oldest siliciclastic tidal deposits (3.2 Ga Moodies Group, South Africa). *Geology* **34**, 253–256.
Onstott TC, Lin LH, Davidson M, Mislowack B, Borcsik M, Hall J, Slater G, Ward J, Sherwood Lollar B, Lippmann-Pipke J, Boice E, Pratt LM, Pfiffner S, Moser D, Gihring T, Kieft TL, Phelps TJ, Vanheerden E, Litthaur D, Deflaun M, Rothmel R, Wanger G, Southam G (2006) The origin and age of biogeochemical trends in deep fracture water of the Witwatersrand Basin, South Africa. *Geomicrobiology Journal* **23**, 369–414.
Parnell J (1999) Petrographic evidence for emplacement of carbon into Witwatersrand conglomerates under high fluid pressure. *Journal of Sedimentary Research* **69**, 164–170.
Pinti DL, Mineau R, Clement V (2009) Hydrothermal alteration and microfossil artefacts of the 3,465-million-year-old Apex chert. *Nature Geoscience* **2**, 640–643.
Rasmussen B, Fletcher IR, Brocks JJ, Kilburn MR (2008) Reassessing the first appearance of eukaryotes and cyanobacteria. *Nature* **455**, 1101–1104.
Robb LJ, Meyer FM (1995) The Witwatersrand Basin, South Africa: Geological framework and mineralization processes. *Ore Geology Reviews* **10**, 67–94.
Schopf JW (1976) Are the oldest 'fossils', fossils? *Orig Life* **7**, 19–36.
Schopf JW (2006) Fossil evidence of Archaean life. *Philosophical Transactions of the Royal Society B* **361**, 869–885.
Schopf JW, Packer BM (1987) Early Archean (3.3-billion to 3.5-billion-year-old) microfossils from Warrawoona Group, Australia. *Science* **237**, 70–73.
Southam G, Donald R (1999) A structural comparison of bacterial microfossils vs 'nanobacteria' and nanofossils. *Earth-Science Reviews*, **48**, 251–264.
Spangenberg JE, Frimmel HE (2001) Basin-internal derivation of hydrocarbons in the Witwatersrand basin, South Africa: evidence from bulk and molecular d13C data. *Chemical Geology* **173**, 339–355.
Steele A, Toporski JKW, Avci R, Guidry S, Mckay DS (2001) Time of flight secondary ion mass spectrometry (ToFSIMS) of a number of hopanoids. *Organic Geochemistry* **32**, 905–911.
Szostak JW, Bartel DP, Luisi PL (2001) Synthesizing life. *Nature* **409**, 387–390.
Tice MM, Lowe DR (2004) Photosynthetic microbial mats in the 3,416-Myr-old ocean. *Nature* **431**, 549–552.
Tissot BP, Welte DH (1984) *Petroleum Formation and Occurrence*, Springer-Verlag, New York, NY.
Ventura GT, Kenig F, Reddy CM, Schieber J, Frysinger GS, Nelson RK, Dinel E, Gaines RB, Schaeffer P (2007) Molecular evidence of Late Archean archaea and the presence of a subsurface hydrothermal biosphere. *Proceedings of the National Academy of Sciences* **104**, 14260–14265.
Waldbauer JR, Sherman LS, Sumner DY, Summons RE (2010) Late Archean molecular fossils from the Transvaal Supergroup record the antiquity of microbial diversity and aerobiosis. *Precambrian Research* **169**, 28–47.